https://doi.org/10.5194/essd-2023-236
Preprint. Discussion started: 26 July 2023

Open Access Earth System Science Data Discussions

Monitoring the regional Ocean Heat Content change over the Atlantic Ocean with the space geodetic approach

Victor Rousseau[1], Robin Fraudeau[1], Matthew Hammond[2], Odilon Joël Houdegnonto[3,4,5], Michaël Ablain[1], Alejandro Blazquez[6], Francisco M. Calafat[7], Damien Desbruyères[3], Giuseppe Foti[2], William Llovel[3], Florence Marti[1], Benoît Meyssignac[6], Marco Restano[8], and Jérôme Benveniste[9]

[1]MAGELLIUM, Ramonville Saint-Agne, 31520, France
[2]National Oceanography Centre, Southampton, United Kingdom
[3]Univ Brest, CNRS, Ifremer, IRD, Laboratoire d'Océanographie Physique et Spatiale (LOPS), IUEM, F29280, Plouzané, France
[4]Jet Propulsion Laboratory, California Institute of Technology, Pasadena, CA 91109, United States of America
[5]International Chair in Mathematical Physics and Applications (ICPMA-UNESCO Chair), University of Abomey-Calavi, Benin
[6]LEGOS, Université de Toulouse, CNES, CNRS, UPS, IRD, 31000, Toulouse, France
[7]National Oceanography Centre, Liverpool, United Kingdom
[8]SERCO-ESRIN, Frascati, 00044, Italy
[9]ESA/ESRIN, Frascati, 00044, Italy

Correspondence: Victor Rousseau (victor.rousseau@magellium.fr)

Abstract. The estimation of the regional Ocean Heat Content (OHC) is essential for climate analysis and future climate predictions. In this study, we propose a method to estimate and propagate uncertainties in regional OHC changes. The OHC is estimated with space geodetic steric data corrected from salinity variations estimated with in situ measurements. A variance-covariance matrix method is used to propagate uncertainties from space geodetic data to the OHC change. The integrated OHC change over the Atlantic basin is 0.17 W m^{-2} which represents 21% of the global OHC trend, with significant trends observed in 52% of the Atlantic basin. Uncertainties in OHC trends are mainly attributed to manometric sea level change uncertainties. We validate our space geodetic OHC estimates at two test sites, representing the subtropical and subpolar regions of the North Atlantic, highlighting their importance in understanding climate dynamics. Our results show good agreement between space geodetic estimates and in situ measurements in the North Atlantic region. The space geodetic OHC trends reveal a warming pattern in the southern and western parts of the North Atlantic, particularly in the Gulf Stream region, while the northeastern part exhibits cooling trends. Overall, our study provides valuable insights and a new framework to estimate regional OHC change and its uncertainties, contributing to a better understanding of the Earth's climate system and its future projections. The space geodetic OHC change product (version 1.0) is freely available at https://doi.org/10.24400/527896/a01-2022.012 (Magellium/LEGOS, 2022).

https://doi.org/10.5194/essd-2023-236
Preprint. Discussion started: 26 July 2023

Open Access Earth System Science Data Discussions

1 Introduction

Due to its large volume and its high thermal inertia, the ocean accounts for most of the planetary heat uptake generated by the Earth Energy Imbalance (EEI) associated with the current climate change ($\simeq 91\% \pm 2\%$, Church et al., 2011; Levitus et al., 2012; Meyssignac et al., 2019; von Schuckmann et al., 2020). The ability of the ocean to store and redistribute this excess heat plays a key role in the long-term transient response of the Earth system to climate change (Rose and Rayborn, 2016).

The global Ocean Heat Content (OHC) change is the dominant term in the planetary energy budget on timescales longer than several months and can be considered a proxy for Earth's net radiative flux imbalance. As it integrates the full ocean it is significantly more representative of EEI than the global surface temperature changes (Palmer et al., 2019; von Schuckmann et al., 2016). Earlier studies have proposed an accurate monitoring and description of the global and full-depth OHC change (Desbruyères et al., 2017; Meyssignac et al., 2019; von Schuckmann et al., 2020; Hakuba et al., 2021; Marti et al., 2022). At regional scales, however, this description remains more limited.

At regional scales, the spatial pattern of ocean warming affects the strength of climate feedbacks and climate sensitivity (Rose et al., 2014; Rose and Rayborn, 2016), which in turn determine the asymptotic response of the global surface temperature of the climate system for a given increase in CO_2 concentrations. Understanding and accurately monitoring the patterns of OHC change from the global to regional scales are therefore of central importance to constraining properly climate parameters of key importance such as climate sensitivity (Chenal et al., 2022).

In the North Atlantic, changes in the transport and storage of heat play a key role in both global and regional scale climate changes. At the global scale, such changes are crucial to the dynamics of the global overturning circulation, including the global ocean deep water circulation, which partly modulates the rate of vertical diffusion of the excess heat into the ocean on climate time scales (Gnanadesikan, 1999). On a regional scale, they are important because a large part of the heat transport from the tropics to higher latitudes takes place in the first layers of the ocean, interacts with the atmosphere and probably modulates the variability of the climate in Western Europe (Palter, 2015).

The OHC can be inferred by several approaches each with their own advantages and limitations (Meyssignac et al., 2019). The first approach involves using direct in situ measurements of temperature and salinity such as those made autonomously by the Argo network of profiling floats (von Schuckmann et al., 2020). These in situ measurements are unevenly distributed in both space and time, with still poor sampling of the deep ocean (below 2000m), marginal seas, coastal regions and below sea ice. The second approach consists in using direct satellite measurements of net ocean surface heat fluxes (Kato et al., 2018; L'Ecuyer et al., 2015). These net fluxes are estimated from the satellite observations of radiative and turbulent fluxes. However, this approach is associated with large residuals and uncertainties and at regional scales the fluxes need to be corrected from horizontal energy transport by ocean dynamics (Meyssignac et al., 2019). A third approach is to use ocean reanalyses with assimilation of satellite and in situ observations (Stammer et al., 2016). Some reanalyses (such as ECCOv4, Forget et al., 2015; ECCO Consortium et al., 2020) are dynamically consistent but they can be numerically biased in regions with sporadic spatio-temporal observational constraints such as polar regions or the deep ocean (Palmer et al., 2017). The fourth approach is the space geodetic approach which consists in measuring sea level changes due to thermal expansion and saline contraction of the

https://doi.org/10.5194/essd-2023-236
Preprint. Discussion started: 26 July 2023

ocean (steric sea level change) based on differences between total sea level changes derived from altimetry measurements and manometric sea level changes derived from gravimetry measurements. This approach offers consistent temporal and spatial sampling of the ocean, integrated over the entire ocean water column, with nearly a global coverage of the oceans, except for polar regions above 82°. But it does not provide separated estimates of the contributions of different ocean layers to the total OHC change.

At global scale, salinity has a negligible influence on the total sea level (Gregory et al., 2019). The potential of the geodetic approach to estimate the global thermal expansion and the global OHC change at global scale has been demonstrated (Marti et al., 2022; Hakuba et al., 2021). A key advantage of this method is its ability to provide a realistic estimation of the uncertainties from time correlated errors.

At regional scales, the influence of salinity on the total sea level is not negligible anymore (Llovel and Lee, 2015) and needs to be accounted for. In this case, the thermal expansion is obtained by subtracting halosteric variations due to salinity change derived from in situ measurements from the regional steric sea level derived from the space geodetic approach. A preliminary estimate of the OHC change at regional scales was done with the geodetic approach (Marti et al., 2022) over 2002-2016 but the uncertainty was just estimated for the global ocean and not at the regional scale. Furthermore, they did not remove the halosteric variations to estimate the OHC change. Here we propose a new estimate of the regional changes in OHC in the Atlantic ocean with an estimate of the regional uncertainties. The originality of the present study lies in the provision of OHC change at regional scales with a combination of space geodetic and in situ data to correct for the salinity effect. Combining regionally space geodetic with in situ data has three major advantages: 1) it provides an estimate of the thermosteric sea level change integrated over the full ocean depth; 2) it provides a very good spatial and temporal coverage of the ocean since April 2002; and 3) it provides an estimate of the uncertainties from the altimetry and gravity measurements.

The physical assumptions behind the estimation of the OHC change are given in section 2. Section 3 describes the datasets used for the estimation of the OHC change and its validation. The preprocessing of the datasets used for the computation of OHC is explained in section 4. A subsection is specially dedicated to the validation of the estimation of steric sea level change from the space geodetic approach. Another subsection is dedicated to the description of the method used to propagate uncertainties. Results are presented in section 5. A validation work was also performed with in situ products (section 6). Finally, conclusions and perspectives are given in section 7.

2 Physical principle of the OHC change calculation

In the space geodetic approach, the OHC change is estimated from the thermal expansion of the seawater observed from satellite data and in situ data. Thermal expansion corresponds to the change in water density due to temperature change, and is also called TSSL change. The TSSL change is retrieved from the sea level budget equation where the total sea level change (ΔSL) is the sum of the manometric sea level (ΔMAN) and the steric sea level change (ΔSSL) expressed in meters. The latter can be decomposed in two terms, the thermal expansion change ($\Delta TSSL$) and the halosteric sea level change ($\Delta HSSL$). Thermal

https://doi.org/10.5194/essd-2023-236
Preprint. Discussion started: 26 July 2023

expansion is derived at every timestep and spatial coordinate following Eq. (1):

$$\Delta TSSL(lon,lat,t) = \Delta SL(lon,lat,t) - \Delta MAN(lon,lat,t) - \Delta HSSL(lon,lat,t) \quad (1)$$

The TSSL change is converted into OHC change with the use of the Integrated Expansion Efficiency of Heat (IEEH) coefficient. This coefficient expresses the ratio of the thermosteric sea level over the heat content. It is estimated from direct measurements of TSSL and OHC from in situ data. It is expressed as in Eq. (2):

$$IEEH(lon,lat,t) = \frac{\Delta TSSL(lon,lat,t)}{\Delta OHC(lon,lat,t)} \quad (2)$$

where TSSL, the thermosteric sea level referenced to a physical thermosteric sea level (defined at 0° Celsius and 35 PSU), and OHC, the ocean heat content, are both integrated over the whole water column.

With the estimate of TSSL change and IEEH, the regional OHC change is calculated following a regional version of the geodetic approach from Marti et al. (2022). OHC change (ΔOHC) at a specific longitude (lon), latitude (lat) and time (t) is defined by the difference between OHC at t and $t0$, and can be written as in Eq. (3):

$$\Delta OHC(lon,lat,t) = \frac{1}{S_{cell}(lon,lat)} \left[\frac{\Delta TSSL(lon,lat,t) + TSSL(lon,lat,t0)}{IEEH(lon,lat,t)} - \frac{TSSL(lon,lat,t0)}{IEEH(lon,lat,t0)} \right] \quad (3)$$

The OHC change will be given in J/m^2 where the S_{cell} is the sea surface of interest in m^2.

In this study, TSSL change is derived from SL change, which is observed from space with radar altimetry missions (section 3.1), MAN change is observed from space with space gravimetry missions (section 3.2) and HSSL change is observed from in situ observations of ocean temperature and salinity (section 3.3.1). In situ datasets of temperature and salinity are also used to estimate the regional IEEH (section 3.3.2).

3 Data

3.1 Total sea level change

The total sea level change at regional scales is derived from the sea level products operationally generated by the Copernicus Climate Change Service (C3S). This dataset, fully described in Legeais et al. (2021) is highly stable and specifically designed for climate applications. It provides daily sea level anomalies grids at a 1/4° spatial resolution. It is based on reference altimeter missions (TopEx/Poseidon, Jason-1,2,3 and S6-MF very soon). Complementary missions (ERS-1,2, Envisat, Cryosat, SARAL/Altika, Sentinel-3A) are used to increase spatial coverage. C3S provides total sea level anomalies (SLA) around a mean sea surface (MSS) above the reference mean sea-surface computed over 1993-2012. The C3S sea level grids were also corrected for the glacial isostatic adjustment (GIA) applying a regional correction from an ensemble average of 27 ICE-5G model viscosity variations (Spada and Melini 2019). A correction of +0.1 mm/yr is also applied for the deformations caused by the modern melt of land ice (GRD) on the ocean crust (Frederikse et al., 2017; Lickley et al., 2018).

https://doi.org/10.5194/essd-2023-236
Preprint. Discussion started: 26 July 2023

The altimetry sea level uncertainties are provided at regional scales by Prandi et al. (2021). Uncertainties are characterised for the main sources of errors including high frequency noise from orbit determination and geophysical corrections, low frequency noise from the wet troposphere correction and drifts from the GIA correction.The uncertainties account for time correlation in errors. However, to date, the spatial correlation of the sea level errors has not been described.

3.2 Manometric sea level change

GRACE and GRACE Follow On (GRACE-FO) missions allow the monitoring of ocean mass change from gravity measurements. It is used to derive the manometric component of the sea level from 04/2002 to nowadays. As GRACE decommissioned in 2017, and its successor GRACE-FO was launched in May 2018, there is a 11 months data gap in 2017/2018. In this study we considered an update of Blazquez et al. (2018) ensemble of GRACE solutions (http://ftp.legos.obs-mip.fr/pub/soa/gravimetrie/grace_legos/V1.5.1). This ensenble is based on normalised spherical harmonic solutions from six different centres and a large variety of post-processing corrections including corrections for the geocentre motion, the oblateness of the Earth, the dealiasing of ocean and atmosphere, the filtering of the noise linked to the so-called stripes of GRACE gravity data, the GIA and the leakage correction. In comparison with the ensemble V1.4 used in Marti et al. (2022), the ensemble V1.5.1 accounts for 288 solutions, notably because it includes a new geocentre solution (Dahle et al., 2013). There is also an increase in the temporal coverage in the new version of the ensemble as the data gap between GRACE and GRACE-FO has been reduced. Two extra corrections were also added: one for the earthquakes (Tang et al., 2020) and one for the ocean mass change at the first 300km near Greenland and Antarctica. In MAN grids we fill in the data gap which is present between July 2017 and June 2018 with a cubic approximation that is applied regionally on deseasonned and detrended time series.

We use the Blazquez et al. (2018) ensemble to estimate the variance-covariance matrix that characterises the MAN uncertainties. This method accounts for spatio-temporal correlated errors of the MAN that are implicitly included in the ensemble.

3.3 In situ data

3.3.1 Halosteric sea level change

The halosteric sea level (HSSL) change is estimated from in situ temperature (T) and salinity (S) data. The computation of the sea level variations due to salinity variations relies on the thermodynamic equation of seawater (McDougall and Barker, 2011). The HSSL component is estimated from the combination of two in situ temperature and salinity datasets. From 0 m to 2000 m depth, the HSSL is calculated with the ISAS20 temperature and salinity datasets (Kolodziejczyk et al., 2021). The ISAS procedure and product is described in (Gaillard et al., 2016). It is based on the measurements from the Argo and Deep Argo floats (note that at the time of the ISAS20 computation, few of Deep Argo profiles reached the data quality standard required to be implemented into the optimal interpolation tool, personnal communication from Nicolas Kolodziejcyk). Between 2000m and 6000m, HSSL is calculated with EN4.2.2.l09 temperature and salinity gridded fields (Good et al., 2013; Levitus et al., 2009). EN4.2.2.l09 product has been chosen to address the deep ocean contribution as it relies on data from other ocean observing systems, such as moored buoys and research vessels (Good et al., 2013). Note that deep ocean measurements remain sporadic

https://doi.org/10.5194/essd-2023-236
Preprint. Discussion started: 26 July 2023

both spatially and temporally so that most of the deep ocean signal remains close to the climatology after optimal interpolation. T and S fields from ISAS20, which were used to estimate halosteric change and IEEH are given at a 1/2° resolution whereas EN4.2.2.l09 fields are given at a 1° resolution. Before merging the two HSSL contributions, the HSSL based upon ISAS20 is first interpolated at a 1° resolution.

Recent studies highlight that in situ salinity datasets from Argo present a drift since 2016 due to anomalies on conductivity sensors (Wong et al., 2020). Barnoud et al. (2021) showed that this drift affects the global mean HSSL estimates. The impact of this halosteric drift on the regional OHC change is still unknown and difficult to quantify.

Currently the only uncertainties associated with HSSL that are available are formal uncertainties from temperature and salinity profiles estimated in EN4.2.2.l09 and ISAS20 datasets. In this present study, these uncertainties have not been propagated to the HSSL change.

3.3.2 IEEH

The IEEH is also computed with the combination of ISAS20 and EN4.2.2.l09 in situ datasets which were already depicted in section 3.3.1. First we compute the thermal expansion (TSSL) and Ocean heat content change (OHC change) from T and S based on TEOS-10. The high frequencies of TSSL and OHC changes are removed by locally applying a low-pass filter (Lanczos) with a cutoff period of 3 years before estimating the IEEH. This high-frequency variability can arise from various sources, such as local weather conditions, ocean currents, and internal ocean waves. These high-frequency signals can mask the underlying signal of interest, which is the relationship between interannual to long-term variability in ocean thermal expansion and thermosteric sea level.

To propagate and estimate the uncertainties on the regional OHC change from the space geodetic data, the uncertainty of the IEEH must be taken into account. We use the IEEH uncertainty estimated at global scale in Marti et al. (2022) and apply it everywhere as a constant. The global estimate results from the dispersion between several global IEEH estimated from 11 Argo solutions (see Marti et al. (2022)). As the IEEH is not an intensive parameter (i.e. it can not be averaged from regional scale to global scale), a scaling factor is used to convert the global uncertainty into regional one with a cross product:

$$e_{IEEH}(lat,lon) = \frac{IEEH(lat,lon) * e_{IEEH_{global}}}{IEEH_{global}} \tag{4}$$

where $e_{IEEH}(lat,lon)$ is the uncertainty at a given latitude and longitude, $IEEH(lat,lon)$ is the values of the regional IEEH, $e_{IEEH_{global}} = 5.5 * 10^{-4} m.YJ^{-1}$ is the uncertainty of the IEEH at global scale (Marti et al., 2022) and $IEEH_{global} = 1.68 * 10^{-25} m.J^{-1}$ is the value of the IEEH calculated at global scale for the in situ product ISAS20-EN4.

3.3.3 Validation products

The space geodetic product is validated in the North Atlantic region at two test sites. First, the product is validated in the subtropical region with two products: an optimal interpolation product based on data from Argo floats and produced by the National Oceanography Centre (hereinafter referred to as NOC Argo OI) and T/S data from RAPID-MOCHA (RAPID-Meridional

https://doi.org/10.5194/essd-2023-236
Preprint. Discussion started: 26 July 2023

Overturning Circulation and Heatflux Array). The NOC Argo OI dataset is a gridded product generated by the NOC using optimal interpolation of Argo profile data including T and S over the depths 0-2000m. The spatial resolution of NOC Argo OI is 1° in latitude/longitude and 20m in depth with a temporal resolution of 10 days. In-situ estimates of depth-integrated OHC were computed from the gridded T and S using thermodynamic routines included in the Gibbs SeaWater (GSW) oceanographic library over the period April 2004 to September 2021. The RAPID programme aims to quantify the Atlantic Meridional Overturning Circulation (AMOC) using an array of moored instruments at a latitude of ∼26.5° N measuring temperature, salinity, and current velocities from the near surface to the sea-floor. Raw instrument mooring data is processed at the NOC and made available as a gridded product, with a 20m spatial resolution, and a 12-hour temporal resolution, currently spanning the period April 2004 to March 2020. The RAPID section was split into two zonal sections demarcated by the full-depth profiles at the Eastern and Western boundaries as well as at the mooring located west of the Mid Atlantic Ridge. OHC was then estimated across each of the two sections using the NOC Argo OI data, calibrated against RAPID observations at the boundaries of each section, relying on the main assumption that the two datasets are equal at these locations except for an additive bias.

The geodetic OHC product is further validated in the Subpolar North Atlantic with two in situ datasets: repeat hydrography along the A25-Ovide section (Mercier et al., 2022) and Argo-based ISAS21 in situ product. OVIDE (Observatoire de la variabilité interannuelle et décennale en Atlantique Nord) consists of 9 Portugal-Greenland hydrography sections occupied every other year during 2002-2018 (in early boreal summer: May-June/June-July). Vertical profiles of T and S, typically spaced out by 20 nautical miles in the interior and down to few nautical miles above steep continental slopes, have been objectively interpolated onto ∼7km x 7km horizontal grid and with a high vertical resolution of 1 m. ISAS21 is an update of ISAS20 that is built with all available Argo and Deep-Argo profiles over the 2002-2020 period (Kolodziejczyk et al., 2021). In the Subpolar North Atlantic, the latitudinal and longitudinal resolution of ISAS21 are ∼0.20° to ∼0.4° and 0.5°, respectively. There are 187 standard depth levels between 0-5500 m depth. Note that prior to the comparison process, all in situ OHC estimates have been regridded onto the horizontal resolution of the space geodetic product (1°x1°). Each time series presented hereafter is an anomaly with respect to its time mean.

4 Data processing

4.1 Propagation of the uncertainties

An added value of this study is to estimate and provide OHC uncertainties at regional scales that take into account the temporal correlation of the space geodetic errors and propagating the uncertainties associated with satellite data to derive regional OHC change uncertainties (Figure C1). This method is an extension of the method proposed by Marti et al. (2022) which had for initial purpose to derive OHC change uncertainties for the global ocean.

The main principle of the method is based on the calculation of the error variance-covariance matrices of the total sea level change ($\Sigma_{SL}(lon,lat,t,t)$), the manometric sea level change ($\Sigma_{MAN}(lon,lat,t,t)$), the halosteric sea level change ($\Sigma_{HSSL}(lon,lat,t,t)$) and to propagate the uncertainties to derive the error variance-covariance matrices (Σ_{OHC}). Here,

https://doi.org/10.5194/essd-2023-236
Preprint. Discussion started: 26 July 2023

$\Sigma_{HSSL}(lon,lat,t,t)$ are neglected, (see section 3.3.1). It might lead to an underestimation of the regional OHC change uncertainties.

The first step to estimate the variance-covariance matrix of OHC uncertainties consists in calculating the error variance-covariance matrices of space geodetic data. $\Sigma_{SL}(lon,lat,t,t)$ is the sum of the individual variance-covariance matrices of each error source from the sea level error budget as in Prandi et al. (2021):

$$\Sigma_{SL}(lat,lon,t,t) = \sum_{i=1}^{n} \Sigma_{Error_i}(lat,lon,t,t) \tag{5}$$

For the manometric sea level change, $\Sigma_{MAN}(lon,lat,t,t)$ is calculated on an annual basis, from the dispersion of the MAN ensemble updated from Blazquez et al. (2018) and described in section 3.2. An additional uncertainty is added in Σ_{MAN} over the GRACE(-FO) data gaps (e.g. between GRACE and GRACE-FO in 2018) to account for sub-annual variability that is not well captured by the gap-filling algorithm (described in section 3.2).

For each latitude and longitude of the MAN ensemble, the regional variance-covariance matrix is computed using all the solutions of the ensemble. The resulting MAN ensemble solutions contains n temporal vectors noted hereafter Xi for i from 1 to n. The MAN variance-covariance matrix reads:

$$\Sigma_{MAN}(i,j)(lat,lon,t,t) = cov(X_i,X_j)(lat,lon,t,t) = E[(X_i - E[X_i])(X_j - E[X_j])](lat,lon,t,t) \tag{6}$$

The second step consists in calculating the variance-covariance matrices of the TSSL change. Since TSSL is the differences between SL, MAN and HSSL, Σ_{TSSL} is obtained by summing the variance-covariance matrices of the errors of SL, MAN and HSSL:

$$\Sigma_{TSSL} = \Sigma_{SL} + \Sigma_{MAN} + \Sigma_{HSSL} \tag{7}$$

Note that Equation 7 implicitly assumes that the errors of SL, MAN and HSSL are uncorrelated with each other. However, in practice a few similar geophysical corrections are applied on both SL and MAN which can generate correlated errors not quantified to date. However, we expect these correlated errors to be small because the system error measurements are independent and there are few potential sources of correlated errors (e.g. GIA and ocean tide). Moreover, if observing systems are different and do not allow the observation of the ocean with the same spatio-temporal sampling, errors could be introduced while interpolating these datasets to the same spatio-temporal resolution. The study of the uncertainties associated with this source of error has not been quantified yet.

The third step consists in propagating the uncertainties in the calculation of the OHC change. The OHC is derived from the TSSL change divided by the IEEH. Considering their respective uncertainties, we have:

$$\Delta OHC(t,lat,lon) = \frac{\Delta TSSL(t,lat,lon) \pm e_{TSSL}(t,lat,lon)}{IEEH(t,lat,lon) \pm e_{IEEH}(lat,lon)} \tag{8}$$

Assuming TSSL and IEEH uncorrelated, the variance-covariance matrix of the OHC (Σ_{OHC}) can be estimated using the following equation (see Taylor (1997), Eq. 3.8):

$$\Sigma_{OHC} = \frac{1}{IEEH^2}\Sigma_{\Delta TSSL} + (\frac{IEEH}{e_{IEEH}})^2 \Delta OHC.\Delta OHC^t \tag{9}$$

https://doi.org/10.5194/essd-2023-236
Preprint. Discussion started: 26 July 2023

The uncertainty on trends or acceleration can be estimated for any time span from the variance-covariance matrix (Σ), The mathematical formalism is fully described in Ablain et al. (2019). It consists in fitting the trend and the acceleration from a linear regression model ($y = X\beta + \epsilon$) applying an ordinary least square (OLS) approach, where the estimator of β with the OLS, noted $\hat{\beta}$ takes into account Σ and follows a normal law :

$$\hat{\beta} = N(\beta, (X^t X)^{-1}(X^t \Sigma X)(X^t X)^{-1}) \tag{10}$$

4.2 Space geodetic SSL change

A processing chain was specifically developed in order to calculate the OHC change from space geodetic measurements and in situ products, following the physical principle from section 2. The first step consists in pre-processing the grids of input data over the full period. All grids are interpolated on a 1° and a monthly resolution. The space geodetic approach gives the estimation of the SSL change following :

$$\Delta SSL(lon, lat, t) = \Delta SL(lon, lat, t) - \Delta MAN(lon, lat, t) \tag{11}$$

Then, Atlantic Ocean trends of the dilatation of seawater are estimated from April 2002 to December 2020 following the mathematical statement in section 4.1.

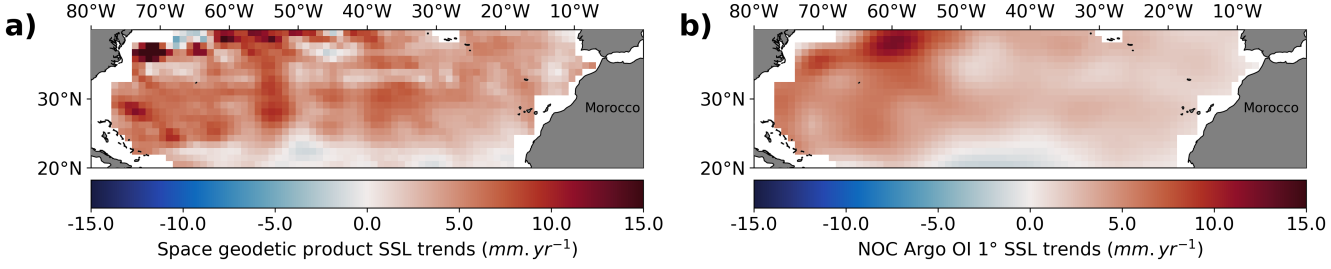

Figure 1. (a) SSL trends in each 1° grid cell of the Subtropical North Atlantic region for the space geodetic product, (b) as for (a) but for NOC Argo OI product.

SSL change from space geodetic data are validated against SSL change estimated with independent in situ data from NOC Argo OI, ISAS21 and OVIDE. Figure 1 shows the validation of the regional steric sea level trends of the space geodetic product against NOC Argo OI product in the Subtropical North Atlantic region. Patterns show overall quite good consistency with the largest values reaching 12 mm yr^{-1} in the NOC Argo OI product against 15 mm yr^{-1} with the space geodetic approach. In both products, weak negative patterns are observed in the southern part of the Subtropical North Atlantic region (-3 mm yr^{-1}). A validation is also carried out in the Subpolar North Atlantic region and along OVIDE section with ISAS21 product. Figure 2 shows that the spatial patterns are in agreement with positive values in the Gulf Stream region reaching 13 mm yr^{-1} for ISAS21 and 15 mm yr^{-1} for the space geodetic product. Negative values are found near Greenland and are less intense in

https://doi.org/10.5194/essd-2023-236
Preprint. Discussion started: 26 July 2023

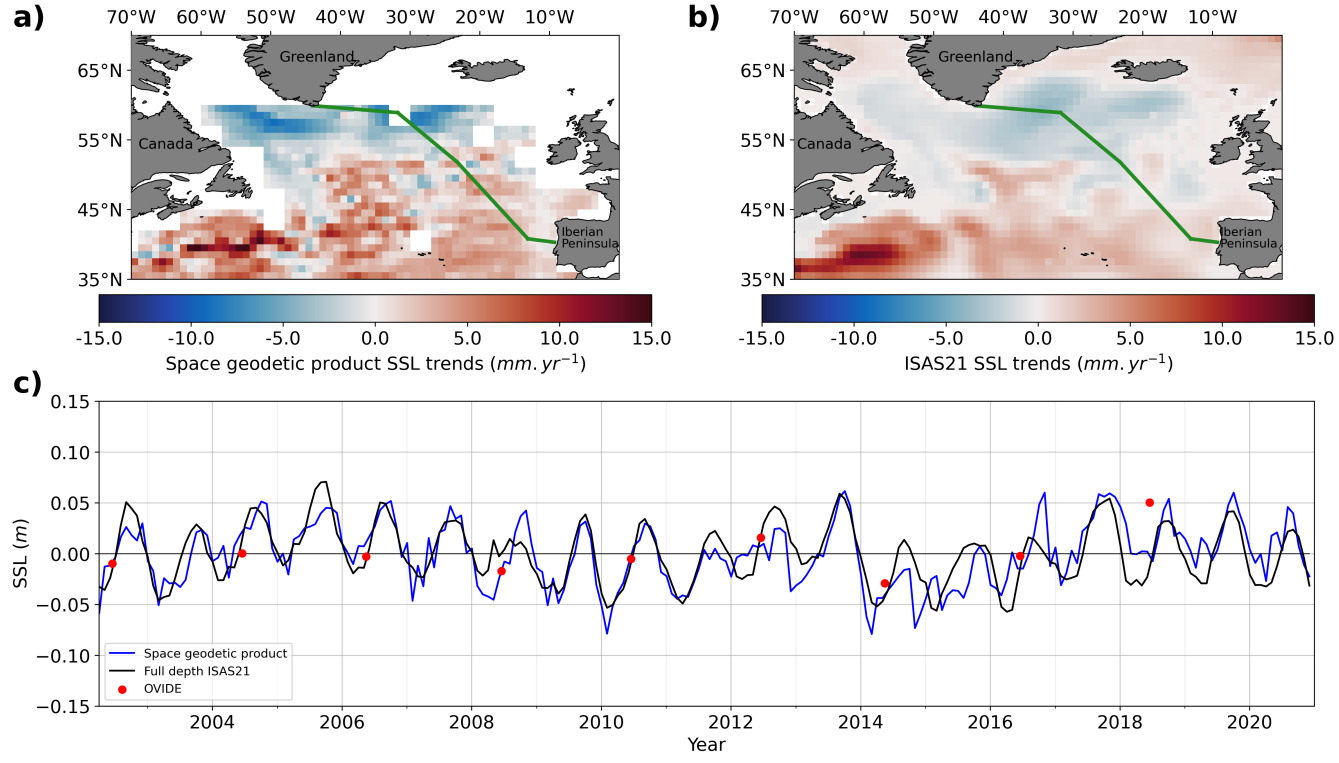

Figure 2. Steric sea level (SSL) trends in the Subpolar North Atlantic (a) from the space geodetic product and (b) from the ISAS21 product. The green line in Figure (a) shows the OVIDE section. (c) Monthly detrended SSL time series along the OVIDE section from the space geodetic product (blue curve), from ISAS21 product (black curve) and from the cruise-based snapshots (red dots).

ISAS21 (-5mm yr^{-1}) than in the space geodetic product (-12mm yr^{-1}). A validation against OVIDE section was also carried out (Figure 2c) and interannual variations of the space geodetic SSL change are found to be close to ISAS21 SSL interannual variations and to OVIDE SSL estimates at the OVIDE section.

4.3 TSSL and OHC change

The TSSL change is calculated from SSL change derived from space geodetic data and HSSL change derived from in situ data (Eq. 1, Figure A1). For the computation of TSSL changes, SSL changes and HSSL changes have to be referenced to the same date. We set arbitrarily the reference date $t0$ to January 2005. SSL and HSSL datasets described in section 3, do not have the same references. The SSL reference is broken down into the SL reference, which is the mean sea surface calculated over 1993-2012, and the MAN solution reference, which is the time average of the ensemble solution over 2005-2015. The HSSL is referenced to a halosteric physical reference (defined at 0° Celsius and 35 PSU). To reference the TSSL change at $t = t0$, we have to apply the following equation for the TSSL change calculation.

https://doi.org/10.5194/essd-2023-236
Preprint. Discussion started: 26 July 2023

$$\Delta TSSL(lon,lat,t) = \Delta SSL(lon,lat,t) - \Delta HSSL(lon,lat,t) - (\Delta SSL(lon,lat,t0) - \Delta HSSL(lon,lat,t0)) \quad (12)$$

Note that we tested the sensitivity to the choice of time reference for TSSL and OHC changes and we found there is no effect on TSSL trends and a weak effect on OHC changes (<1% difference). Once the Thermosteric sea level change has been estimated at regional scale, we estimate the OHC change by using the Argo-derived IEEH coefficient described in section 3.3.2. The spatial coverage of the IEEH is consistent with the one from Marti et al. (2022) which implies a limitation on the spatial coverage of OHC change estimates (Figure B1). Indeed, estimation of temperature and salinity with Argo data is primarily available only in the open ocean , in sea-ice free regions.

The IEEH coefficient can vary over time due to various factors such as changes in ocean circulation, mixing, and stratification especially in regions where mesoscale activity is strong (e.g. western boundary currents regions). The IEEH coefficient can also be influenced by the variability of non-oceanic processes, such as changes in atmospheric conditions and changes in the distribution of sea ice. Although IEEH changes are expected to be small we account for these changes by estimating a time varying IEEH from in situ data. Sensitivity tests made by comparing OHC estimates with constant and time variable IEEH coefficients reveal that in the region of the Gulf Stream the local time-dependency of the IEEH is indeed important to retrieve the local OHC changes. The difference is negligible elsewhere.

In the following, we refer as "space geodetic" OHC change, the OHC derived from this approach that combines total sea level from satellite altimetry , manometric sea level from space gravimetry , halosteric sea level and the IEEH from in situ Argo data. Note that although thus approach is called "space geodetic" approach regionally it depends partly on in situ data.

5 OHC trends over the Atlantic Ocean

Figure 3 shows the OHC trends from the space geodetic method for the period from April 2002 to December 2020. Hatched areas represent non-significant OHC trends (68% confidence level or CL, estimated with the method from section 4.1). On the southern and western part of the North Atlantic, positive trends can reach values up to 15 W m^{-2}, This warming pattern, which is enhanced in the Gulf Stream region, is likely related to a warming of the north atlantic sub-tropical gyre. In the northeastern part of the North Atlantic, OHC trends are negative and reach values down to -13.6 W m^{-2}. This cooling patterns associated to the warming of the subtropical gyre are likely linked to an AMOC-driven reduced oceanic meridional heat transport and the associated redistribution of cold subpolar waters versus warm subtropical waters within its northward-flowing upper limb (Ruiz-Barradas et al., 2018; Desbruyères et al., 2022).

The OHC change integrated over the entire Atlantic basin is 0.17 W m^{-2}. This value is quite similar to the result obtained in a recent study that utilized in situ data, which reported a value of 0.16 W m^{-2} (Desbruyères et al., 2017). The Atlantic basin's OHC change represents approximately 21% of the global OHC change trends. 52% (resp. 32%) of the Atlantic area shows significant trends in OHC at the 68% CL (resp. 90%CL). A major part of the significant trends at the 90% CL are observed in the North Atlantic basin. The uncertainty in OHC trends can reach values up to 3 W m^{-2} in the North Atlantic

https://doi.org/10.5194/essd-2023-236
Preprint. Discussion started: 26 July 2023

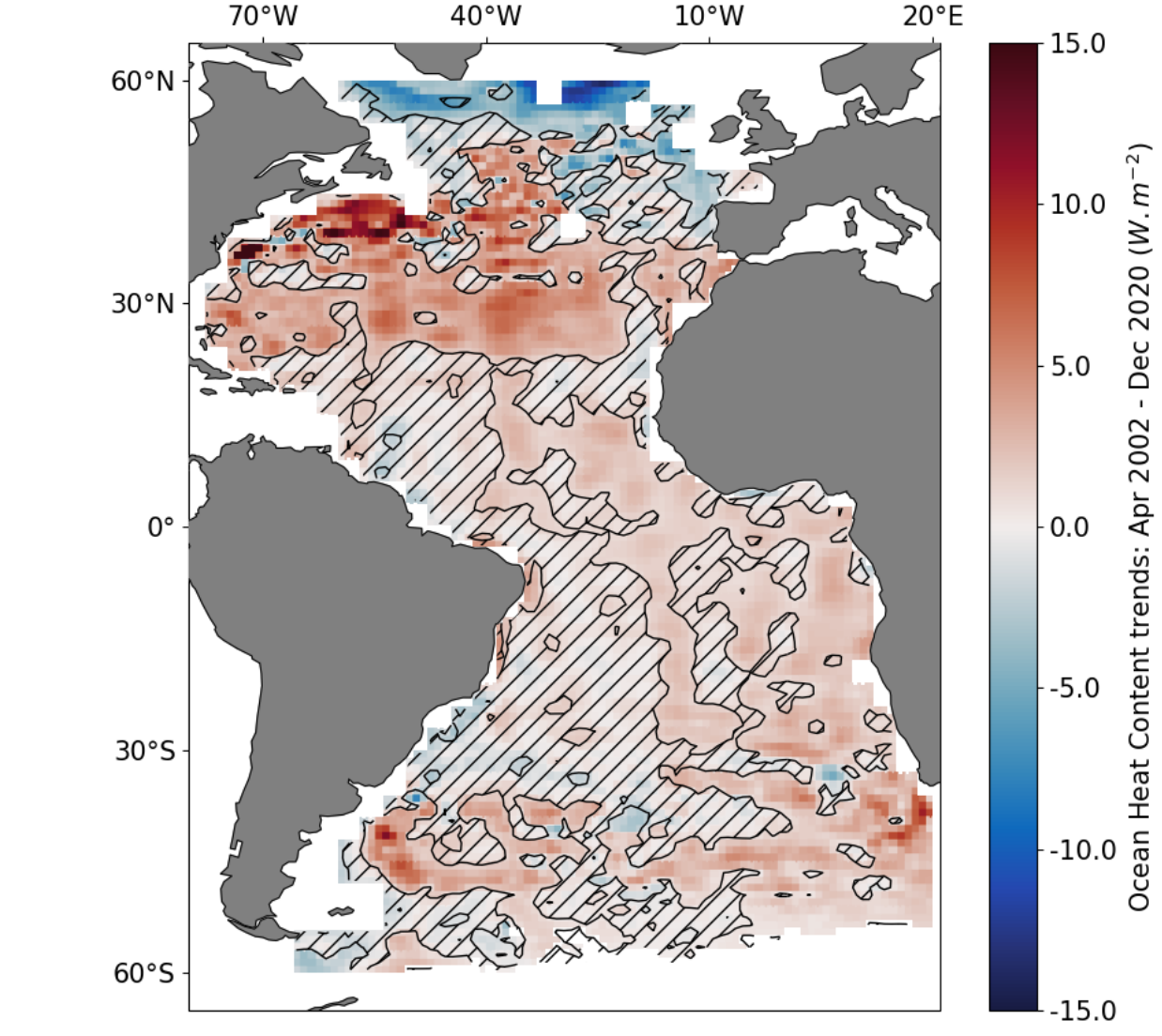

Figure 3. Map of regional OHC change trends on the Atlantic Ocean computed over April 2002-December 2020 with the space geodetic approach. Hatched areas are regions where regional OHC trends are not significant at the 68% confidence level (CL), see section 4.1 for the trends uncertainties calculation. The geographical mask is conditioned by in situ products used to estimate the IEEH.

https://doi.org/10.5194/essd-2023-236
Preprint. Discussion started: 26 July 2023

basin. These OHC trends uncertainties were found to be essentially due to MAN uncertainties with a contribution ranging from 70% at the east of the Atlantic basin to more than 99% at the west of the Atlantic basin (Figure D1). Further investigations need to be conducted to determine which contribution in MAN uncertainties is the highest contributor to OHC uncertainties: the uncertainty due to GIA or to the geocenter realisation.

6 OHC change validation

The OHC change validation aims to provide a detailed experimental error analysis for evaluating the accuracy and reliability of the space geodetic OHC change at two test sites in the North Atlantic region. These two test sites were chosen because they contain independent validation data along the RAPID and OVIDE sections.

6.1 In the Subpolar North Atlantic region

To evaluate the accuracy of the geodetic product in the Subpolar North Atlantic region, the geodetic estimate of the OHC trends are compared to ISAS21 OHC trends (Figures 4a and 4b). The large-scale distribution of OHC trends is consistent in the geodetic and the insitu products with cooling patterns north of 55°N and at the west European basin and warming patterns at 35°-50°N and 70°-30°W. However, both the negative OHC trend in the northern subpolar gyre and the positive OHC trend in the northwestern subtropical gyre appear larger in the geodetic estimate than in the ISAS21 estimate ~-2-5 W m^{-2}. Unraveling the causes of such differences is challenging. They could be due, for instance, to the limited availability of T and S data below 2000m depth in ISAS21, and the relaxation towards the climatology in those deep layers.

Time series of monthly and full-depth OHC interpolated along the OVIDE section during 2002-2020 from both geodetic product and ISAS21 are shown in Figure 4c. The corresponding hydrography-based OHC estimates from the 9 OVIDE hydrography surveys are superimposed (red dots). A good correlation of r = 0.83 (at 95% CL) is found between the full-depth monthly OHC time series, as well as with hydrography-based OHC change estimates from OVIDE dataset (r = 0.6 at 95% CL). However, OHC changes along the OVIDE line appear overestimated in the range of ~-7.5x10^8 to 10^9 J m^{-2} by the space geodetic product in 2008, early 2013, late 2014 to mid 2015 and late 2017 (see the comparison against ISAS21 OHC estimate) and mid 2014 (see the comparison against OVIDE OHC estimate), for instance. Despite these scarce mismatches, consistent OHC trends of -2.15±0.85 W m^{-2} and -2.82±0.66 W m^{-2} are reported for the geodetic product and the in situ ISAS21 estimates along the OVIDE section (Figure 4c).

6.2 In the Sutropical North Atlantic region

OHC trends estimated in each 1° grid cell of the NOC Argo OI dataset are shown in Figure 5b. On the overall, the OHC trends' pattern from the NOC Argo OI dataset are very similar to the geodetic OHC trends' pattern (5a) with an homogeneous positive trend marked in the Northwest by highly positive trends, and in the Northwest and Northeast by slightly negative trends. Additionally, the average magnitude of the space geodetic dataset is very similar to the NOC Argo OI dataset (2.9 W m^{-2} vs 2.3 W m^{-2}), although it does appear to be slightly higher, particularly at latitudes towards the centre of the analysed region.

https://doi.org/10.5194/essd-2023-236
Preprint. Discussion started: 26 July 2023

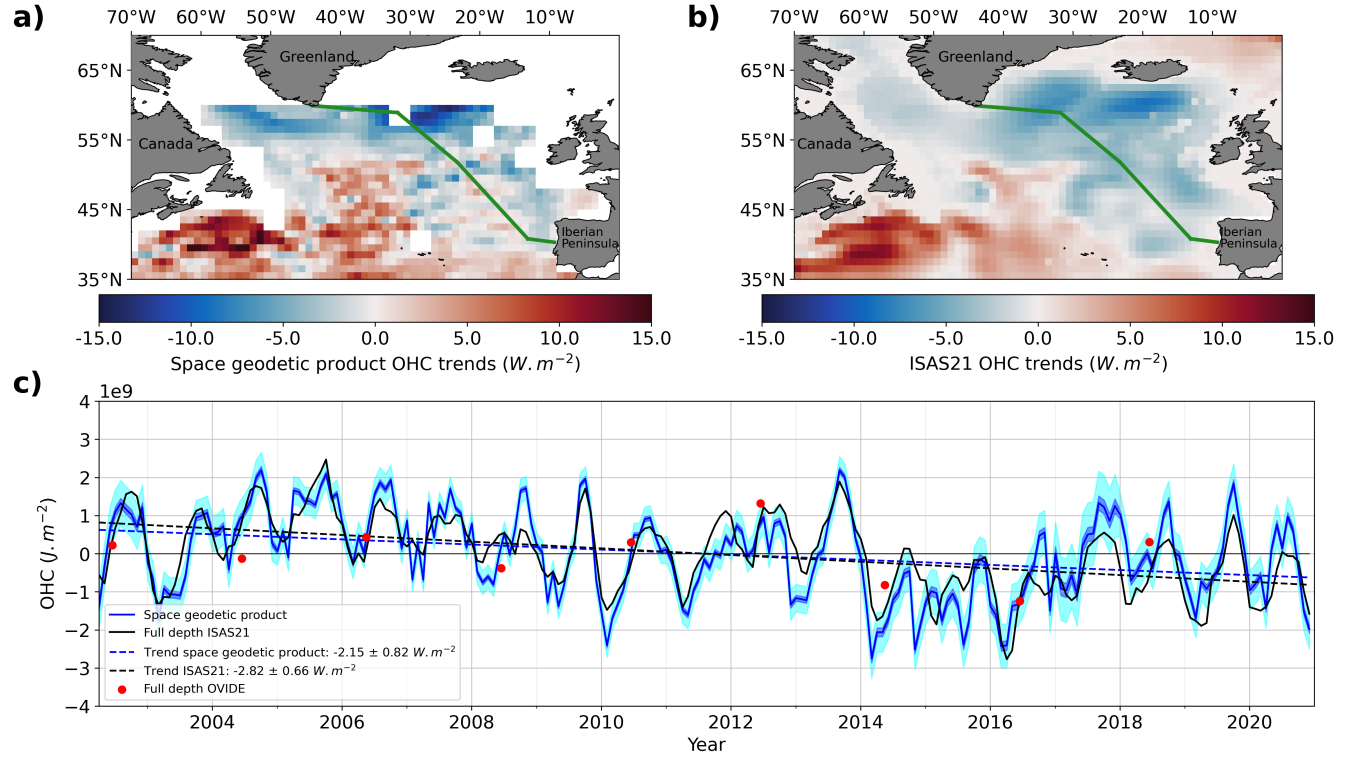

Figure 4. Ocean Heat Content (OHC) trends in the Subpolar North Atlantic (a) from the space geodetic product and (b) from the ISAS21 product. The green line in Figure (a) shows the OVIDE section. (c) Monthly OHC time series along the OVIDE section from the space geodetic product (blue curve), from ISAS21 product (black curve) and from the cruise-based snapshots (red dots). The light blue and cyan bands represent respectively the lower and upper bounds of the error associated with the OHC estimates from the space geodetic product. The dashed blue and black lines are OHC trends lines respectively from the space geodetic and ISAS21 products.

Following the approach described in the methods section, spatially integrated estimates of OHC anomaly were produced across the Western basin of the subtropical North Atlantic at 26.5° N spanning longitudes from 76.74° W to 50.57° W, and across the Eastern Basin between longitudes 50.57° W and 16.23° W. Figure 5c shows the temporal evolution of depth-integrated OHC anomaly estimated from the RAPID array at 26.5°N, spatially integrated across the Western basin of the North Atlantic (black). Equivalent space geodetic OHC anomalies are shown in blue. Trends are shown with dashed lines. The comparison of the RAPID data against space geodetic OHC data reveals fairly good temporal agreement in the OHC time series between both datasets, with trends of 5.21 W m^{-2} and 6.01 W m^{-2} respectively. Using a similar arrangement as the one described above, Figure 5d shows the temporal evolution of OHC anomaly integrated across the Eastern basin calculated using the space geodetic OHC anomalies assessed against RAPID. In general, we observe that temporal agreement with RAPID is somewhat better than that which is found in the Western basin. In comparison with the RAPID-estimated trend of 3.67 W m^{-2}, we find that the space geodetic estimate of 4.12 W m^{-2} is similar but likewise still slightly overestimated. The overall agreement with

https://doi.org/10.5194/essd-2023-236
Preprint. Discussion started: 26 July 2023

340 RAPID is reasonably good for both basins with relative discrepancies between OHC trends derived from space geodetic and from RAPID found to be in the range ∼5-10%.

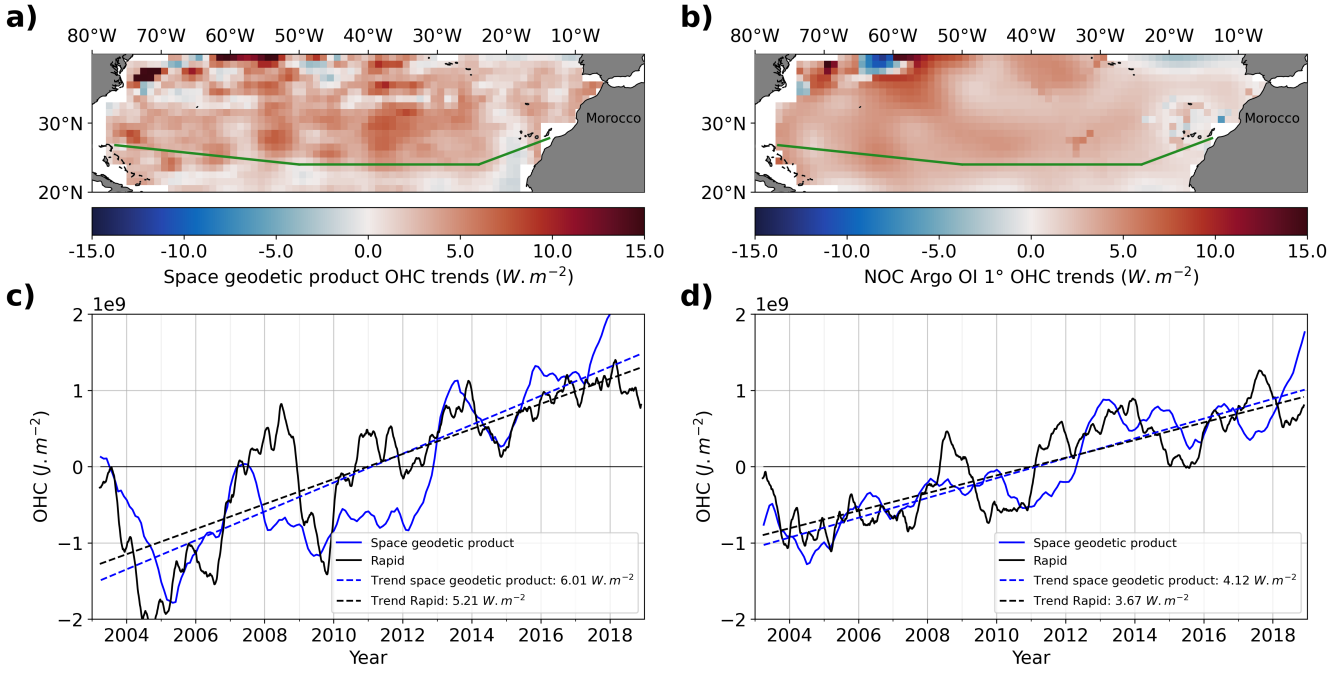

Figure 5. (a) OHC trends in each 1° grid cell of the Subtropical North Atlantic region for the space geodetic product, the green line is indicative of the RAPID-MOCHA mooring array. (b) as for (a) but for NOC Argo OI product. (c) De-seasonalised temporal evolution of depth-integrated OHC anomaly estimated from the RAPID-MOCHA array at 26.5° N in combination with data from the NOC Argo OI product, spatially integrated across the Western basin of the North Atlantic (black). Comparison with estimates from space geodetic OHC anomalies (blue). Respective trends shown with dashed lines. (d) as for (c) but across the Eastern basin of the North Atlantic.

7 Conclusions

The space geodetic approach gives an estimation of the expansion of sea level from space altimetry and space gravimetry measurements over the 19-year period from April 2002 to December 2020. Together with the estimation of the halosteric sea 345 level variations from in situ data, the space geodetic dataset allows to estimate the thermal expansion of the ocean. With the use of the integrated expansion efficiency of heat coefficient derived from in situ data, thermal expansion is converted into an estimation of the ocean heat content.

The estimation of the steric sea level change was first validated with in situ gridded datasets. The results have shown overall good consistency and correlations between the geodetic estimation over the subtropical region with in situ estimation from 350 NOC Argo OI and over the subpolar region with in situ estimation from ISAS21 and OVIDE. The results in terms of ocean

https://doi.org/10.5194/essd-2023-236
Preprint. Discussion started: 26 July 2023

heat content change show that over the full period the trends of the ocean heat content change are significantly strong in the North Atlantic region (up to 15 W m^{-2}). Particularly in these regions, the regional OHC trends show a clear warming over the subtropical region and a cooling over the subpolar region which is in line with patterns derived from the in situ ISAS21 and NOC Argo OI products. Furthermore, the geodetic product was validated in a dedicated section. In the Subpolar North Atlantic, the space geodetic product was compared against hydrography-based OHC along the A25-Ovide repeat hydrography line, as well as against the Argo-based ISAS21 gridded product. The comparison has shown good correlation between their respective OHC estimates (r=0.6, 95% CL for A25-Ovide and r=0.83, 95% CL for ISAS21), including a good match between linear trends. In the Subtropical North Atlantic region, the analysis along the RAPID mooring section has shown fairly good agreement with relative discrepancies in the OHC trends being less than ∼5-10%.

Our study shows that it is essential at regional scale to consider a time varying IEEH for the estimation of the space geodetic OHC change. Indeed, at a regional scale, taking a time constant IEEH is not a valid physical consideration in those regions where the mesoscale activity is strong (e.g. Gulf Stream region, Figures E1 and F1).

This study shows that the combination of spatial data together with in situ data is highly valuable to accurately estimate regional OHC change. However, there are potential issues in the fact of combining space geodetic data and in situ data. In terms of spatial sampling, Argo floats measure ocean variables (e.g., temperature, salinity, and pressure) at discrete locations as they drift with ocean currents. In contrast, space geodetic data, such as satellite altimetry or gravimetry, provides continuous measurements of the full ocean. Those different spatial sampling can lead to biases and data gaps, especially in regions where Argo floats are sparse or absent. One way of assessing this effect would be to use data from a reanalysis subsampled in such a way that mimics the spatio-temporal sampling of the in situ observations, but this is beyond the scope of this paper.

Furthermore, the OHC change is affected by the issues of each one of the product. If Argo floats operate continuously, gravimetry data are affected by scarce gaps of data during the whole period and an even longer gap of data between GRACE and GRACE-FO missions (06/2017-06/2018). In this study, a regional filling gap algorithm was applied to interpolate GRACE data in the gaps. After 2016, the ocean heat content change is also impacted by the spurious drift of conductivity sensors affecting salinity data (Wong et al., 2020; Barnoud et al., 2021). To date, the impact of this drift on regional halosteric change and OHC change has not been investigated yet.

We have developed and presented a new framework for the estimation of regional uncertainties associated with OHC change. This framework allows us to derive realistic OHC uncertainties through a rigorous error budget of the altimetric, gravimetric and in-situ instruments. Currently, most of the uncertainties associated with the geodetic product arise from the uncertainties associated with the manometric component of the sea level and future work is needed to reduce them especially by improving estimates of the geocenter motion and of the GIA. Note that currently, our estimate of the uncertainties is likely underestimated for several reasons. First, the uncertainties are given at annual timescales. A possible improvement would be to provide a variance-covariance matrix at monthly timescales but this might lead to larger variance as variability in the ocean increases with frequency, and is particularly large at mesoscale (1-3 months). Second, uncertainties of halosteric sea level due to salinity variations have not been estimated at regional scale. It has to be estimated properly from temperature and salinity uncertainties in a futur work. Third, the uncertainties of the integrated expansion efficiency of heat (IEEH) have been estimated only at global

https://doi.org/10.5194/essd-2023-236
Preprint. Discussion started: 26 July 2023

scale. A comparison of several Argo products provides an estimate of the regional uncertainty in IEEH due to the differences between different Argo datasets. This comparison shows regional difference in IEEH below 1%. The regional IEEH estimated with the ECCO model is also consistent with IEEH estimates derived from the Argo product. Fourth, the spatial correlation of regional errors has not been described, neither for the altimetry nor for the in situ products.

Efforts made over the Atlantic basin could be pursued by extending the OHC change estimation near coasts but also poleward (up to 82°) which are also key regions for the study of climate change. For the Atlantic area, these zones would represent a gain of surface of around 29%. This could be done by estimating the IEEH from reanalysis data instead of the fully in-situ data based Argo products.

Concerning the scientific perspective, the space geodetic OHC product represents a great opportunity to support operational decadal predictions, but also monitor climate indicators such as the meridional heat transport (MHT). One way to estimate the North Atlantic MHT would be to develop a regional ocean heat budget following Mayer et al. (2022). In situ measurements such as those derived from RAPID section and OSNAP (Overturning in the Subpolar North Atlantic Program) array would complement the results and ultimately allow analysis of MHT variability and investigation of its cause. Applied at all basin scales, the space geodetic approach will support studies on the spatial distribution of energy and the heat transport within the ocean. In combination with Argo estimates of the upper layer OHC, it will also provide estimates of the OHC in deep-ocean layers.

Data availability. OHC change at regional scales or "4DAtlantic" product from space altimetry and space gravimetry was produced by Magellium/LEGOS and distributed by AVISO+ (https://aviso.altimetry.fr) with support from ESA. The results of this study were obtained with the first version of the dataset (V1.0). It is available online at https://doi.org/10.24400/527896/a01-2022.012 (Magellium/LEGOS, 2022). The content of the dataset is described in Table 1. The complete associated documentation is available on the website (experimental dataset description and algorithm theoretical basis document). Further information and documentation are also available on the project website (https://www.4datlantic-ohc.org/).

https://doi.org/10.5194/essd-2023-236
Preprint. Discussion started: 26 July 2023

Table 1. Description of the contents of the dataset.

Variables	Description	Units
time(time)	Time (monthly timestep)	days since 1950-01-01 00:00:00 UTC
time_covar(time_covar)	Time (annual timestep)	days since 1950-01-01 00:00:00 UTC
latitude(latitude)	Latitude of data	degrees_north (°N)
longitude(longitude)	Longitude of data	degrees_east (°E)
crs	Describes the grid mapping used by the 2-D variables of the file	none
cell_surface(latitude, longitude)	Surface of the grid cell	square meter (m^2)
ohc(time, latitude, longitude)	Ocean heat content change	joules per square meter ($J\ m^{-2}$)
ohc_mask	OHC mask to apply on OHC grids for masking interpolated data (1 for observed data and 0 for extrapolated data)	none
ohc_var_covar_matrix (latitude, longitude, time_covar, time_covar)	Variance covariance matrix of errors on OHC change time-series	square joules per meter to the power of 4 ($J^2\ m^{-4}$)
ohc_trends(latitude, longitude)	Trend of the OHC change timeseries	watt per square meter ($W\ m^{-2}$)
ohc_trends_uncertainties(latitude, longitude)	Trend uncertainty of the OHC change timeseries (1-σ)	watt per square meter ($W\ m^{-2}$)

https://doi.org/10.5194/essd-2023-236
Preprint. Discussion started: 26 July 2023

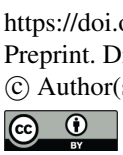

Open Access Earth System Science Data Discussions

Appendix A

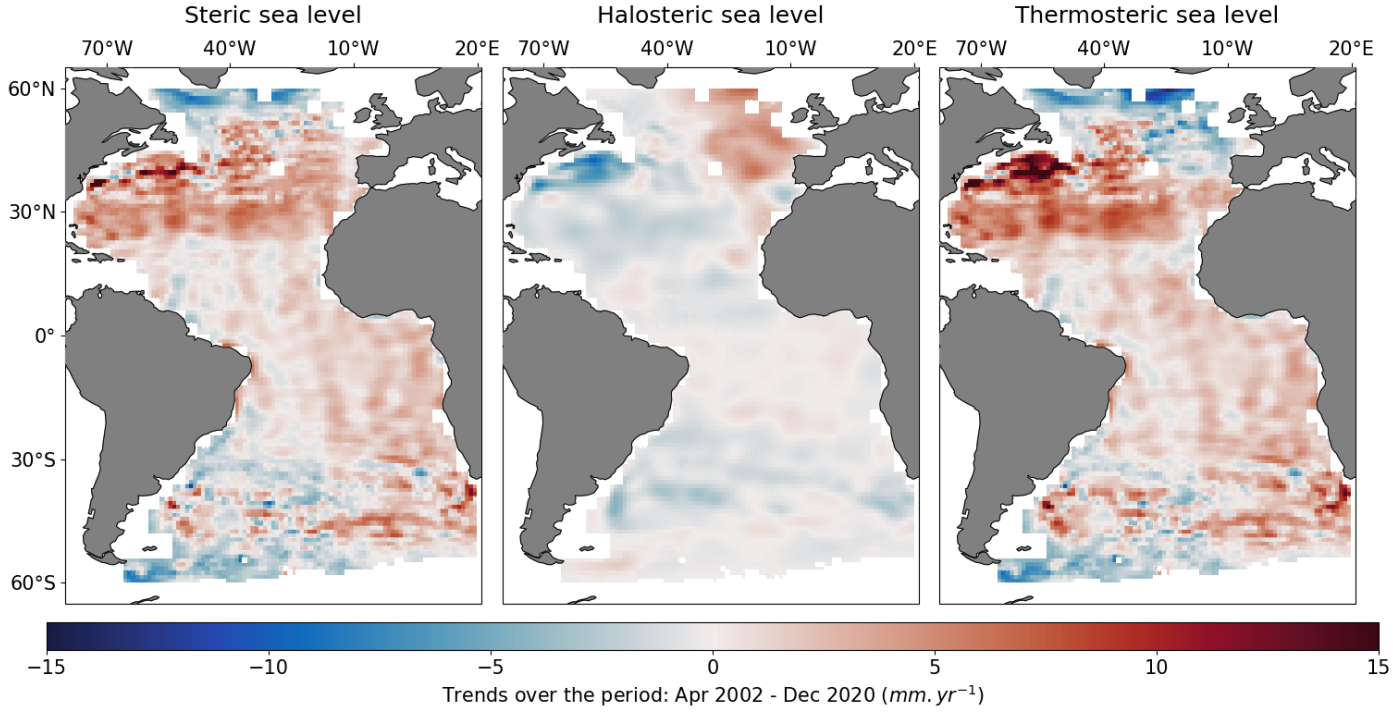

Figure A1. Map of regional trends of steric sea level change estimated with the geodetic approach (left), halosteric sea level change estimated with in situ measurements (center) and their difference which gives an estimate of the thermosteric sea level change (right) on the Atlantic Ocean computed over April 2002-December 2020.

https://doi.org/10.5194/essd-2023-236
Preprint. Discussion started: 26 July 2023

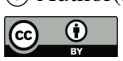

Open Access Earth System Science Data Discussions

Appendix B

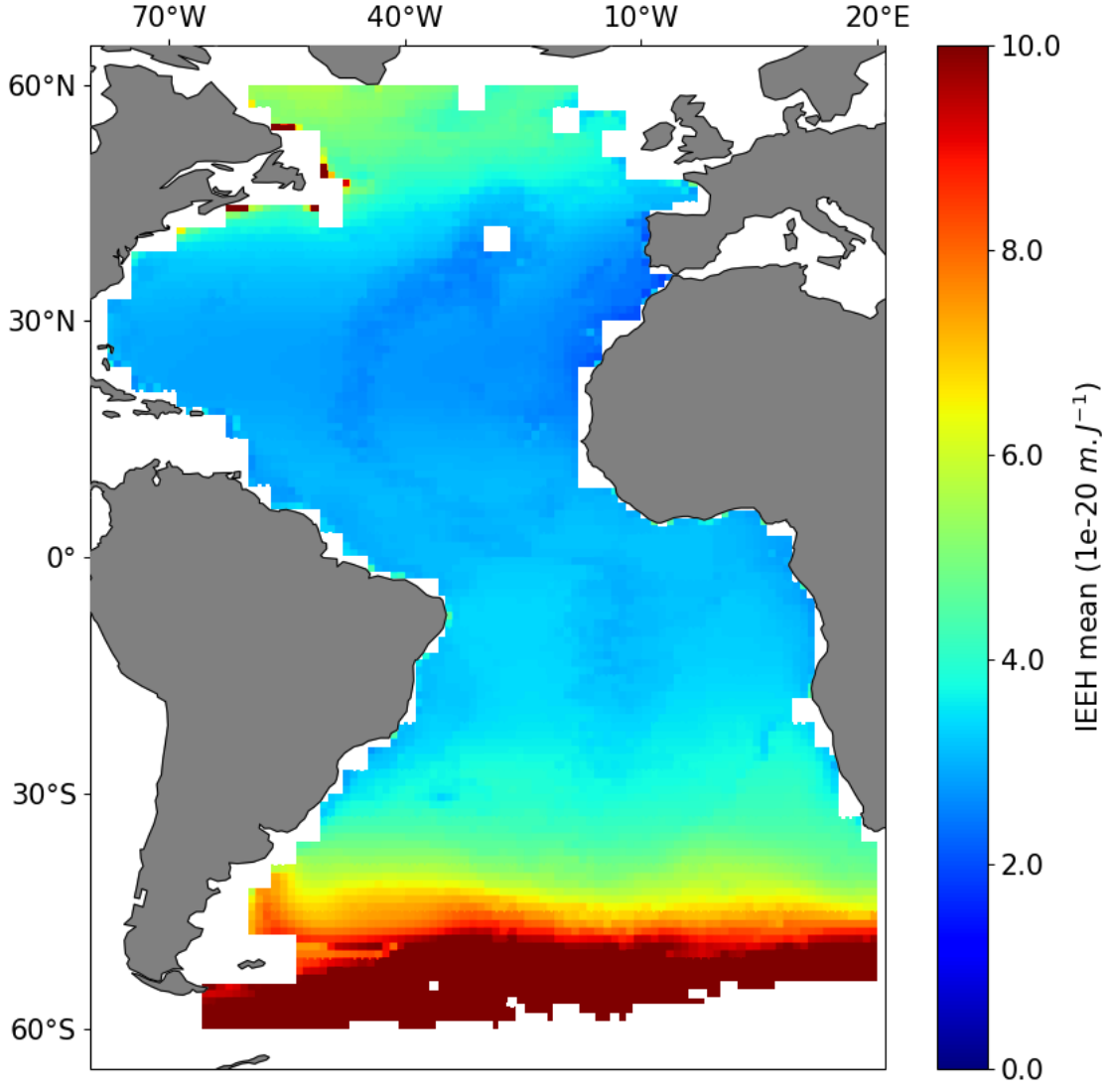

Figure B1. Map of the integrated expansion efficiency of heat (IEEH) time-mean over the Atlantic Ocean over April 2002-December 2020. The IEEH is computed over a spatial extent corresponding to the minimum area of availability of various Argo products (Marti et al., 2022).

https://doi.org/10.5194/essd-2023-236
Preprint. Discussion started: 26 July 2023

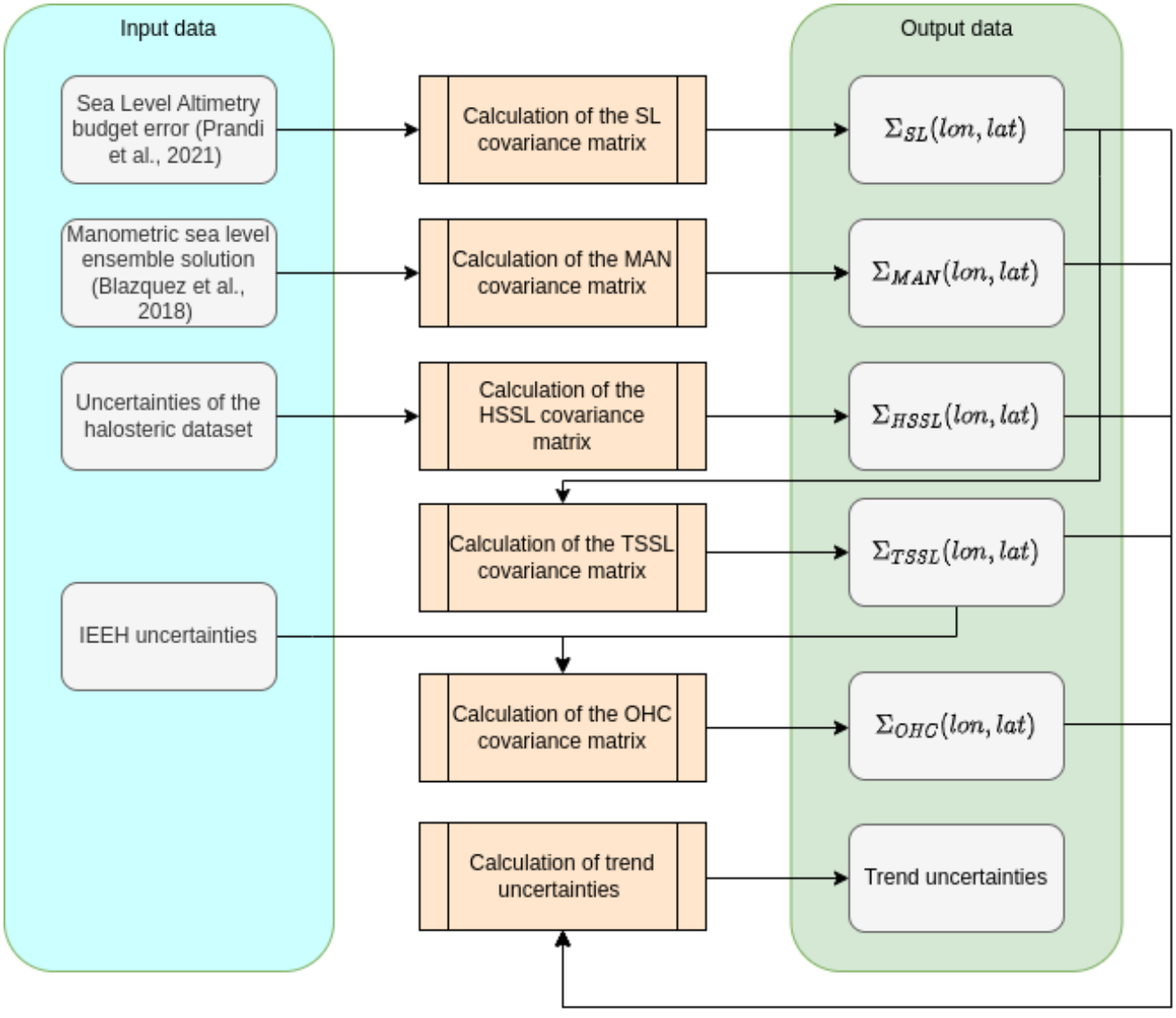

Figure C1. Uncertainty calculation and propagation chain for the ocean heat content (OHC) change estimated with the space geodetic approach.

https://doi.org/10.5194/essd-2023-236
Preprint. Discussion started: 26 July 2023

Appendix D

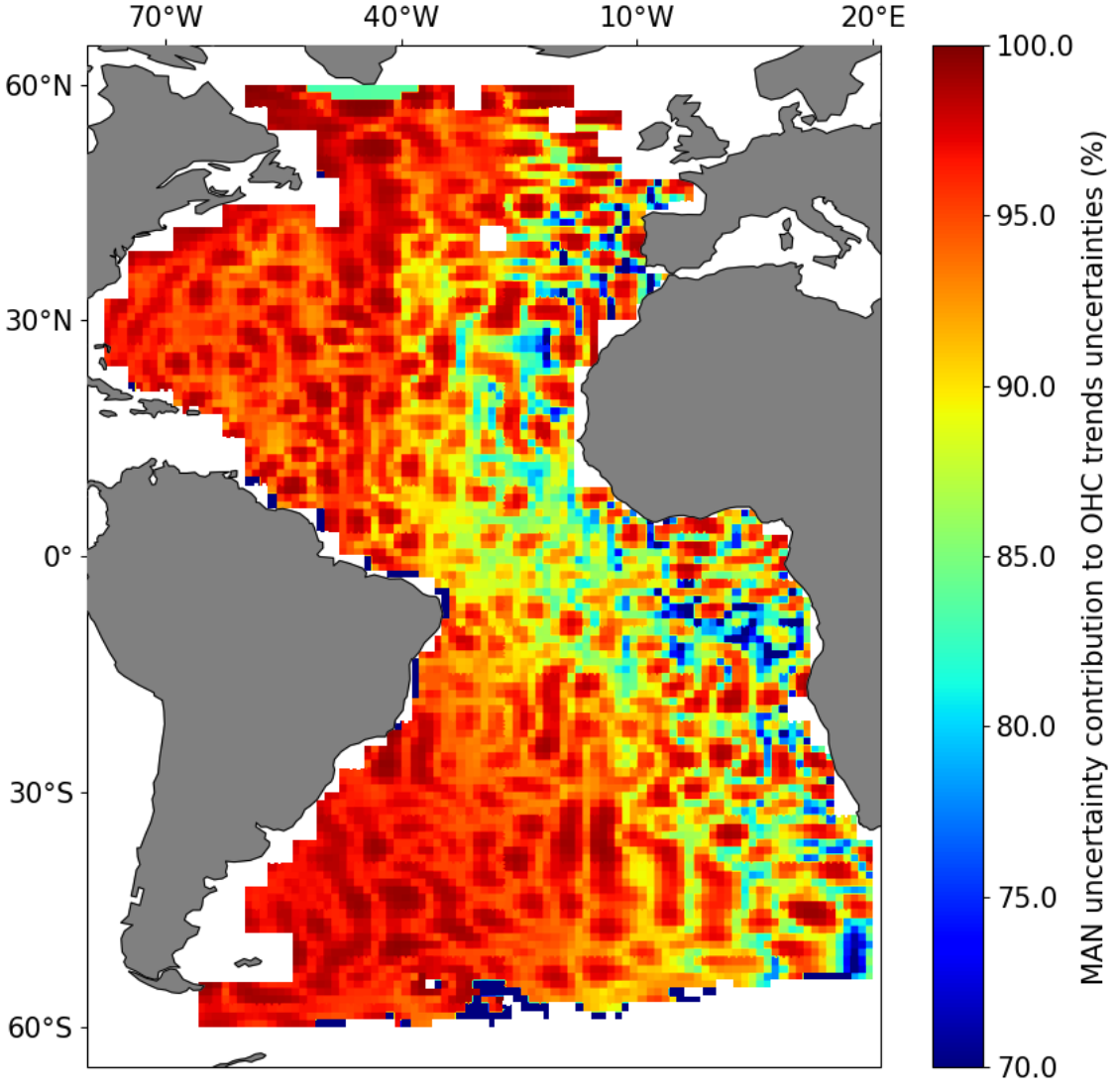

Figure D1. Map of the regional contribution of the manometric component of the sea level (MAN) uncertainties to the ocean heat content (OHC) change trends uncertainties (68% CL).

https://doi.org/10.5194/essd-2023-236
Preprint. Discussion started: 26 July 2023

Open Access Earth System Science Data Discussions

Appendix E

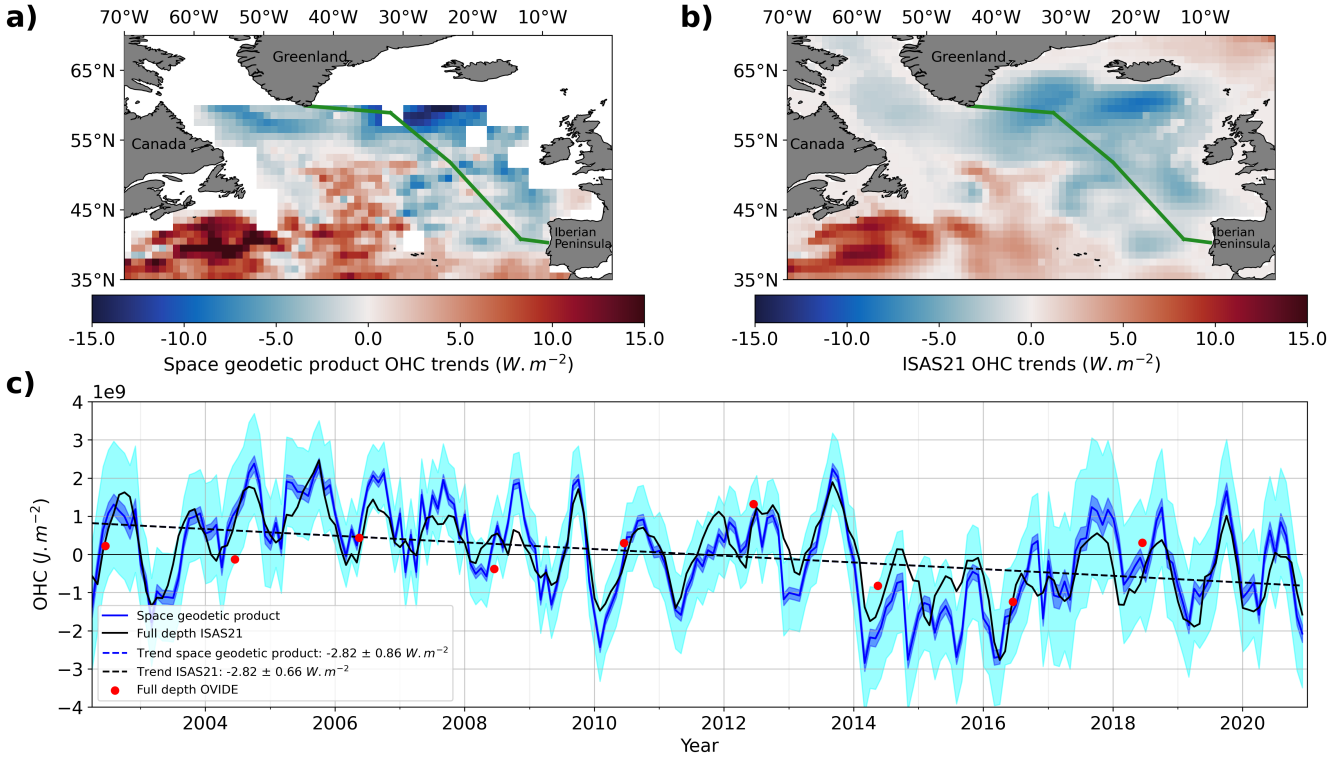

Figure E1. As for figure 4 but the space geodetic product is estimated with a time mean IEEH instead of a time varying IEEH.

https://doi.org/10.5194/essd-2023-236
Preprint. Discussion started: 26 July 2023

Open Access Earth System Science Data Discussions

Appendix F

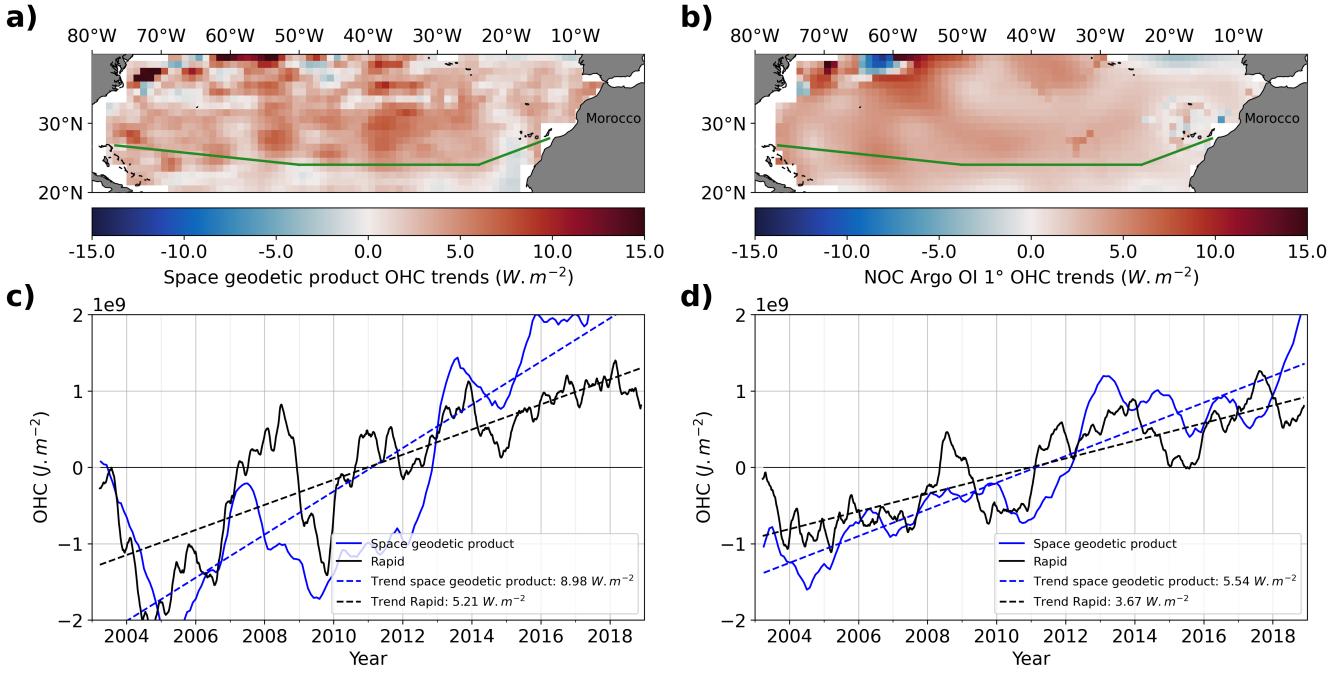

Figure F1. As for figure 5 but the space geodetic product is estimated with a time mean IEEH instead of a time varying IEEH.

https://doi.org/10.5194/essd-2023-236
Preprint. Discussion started: 26 July 2023

Author contributions. VR led and designed the paper. RF focused on the data processing part, OJH and MH respectively focused on the validation part over the subpolar and subtropical regions. MA, AB, FMC, DD, GF, WL, FM, BM made a major contribution in the discussions and revision of the paper. MR and JB reviewed the manuscript and all deliverables of the research project.

Competing interests. The contact author has declared that neither they nor their co-authors have any competing interests.

Disclaimer. Publisher's note: Copernicus Publications remains neutral with regard to jurisdictional claims in published maps and institutional affiliations.

Acknowledgements. We would like to thank all contributors of the 4DAtlantic product. The work was supported by ESA in the frame of the EO4 Society, Atlantic Regional Initiative, 4D-Atlantic-OHC Project (ESA Contract No. 4000134928/21/I-NB). Annaig Prigent (LOPS/IFREMER) is warmly acknowledged for the computation of ISAS21 data set. Anne Barnoud and Julia Pfeffer are also thanked for their feedback on the first draft of this article.

https://doi.org/10.5194/essd-2023-236
Preprint. Discussion started: 26 July 2023

References

Ablain, M., Meyssignac, B., Zawadzki, L., Jugier, R., Ribes, A., Spada, G., Benveniste, J., Cazenave, A., and Picot, N.: Uncertainty in satellite estimates of global mean sea-level changes, trend and acceleration, Earth System Science Data, 11, 1189–1202, https://doi.org/https://doi.org/10.5194/essd-11-1189-2019, publisher: Copernicus GmbH, 2019.

Barnoud, A., Pfeffer, J., Guérou, A., Frery, M.-L., Siméon, M., Cazenave, A., Chen, J., Llovel, W., Thierry, V., Legeais, J.-F., and Ablain, M.: Contributions of altimetry and Argo to non-closure of the global mean sea level budget since 2016, Geophysical Research Letters, https://doi.org/10.1029/2021gl092824, publisher: American Geophysical Union (AGU), 2021.

Blazquez, A., Meyssignac, B., Lemoine, J., Berthier, E., Ribes, A., and Cazenave, A.: Exploring the uncertainty in GRACE estimates of the mass redistributions at the Earth surface: implications for the global water and sea level budgets, Geophysical Journal International, 215, 415–430, https://doi.org/10.1093/gji/ggy293, 2018.

Chenal, J., Meyssignac, B., Ribes, A., and Guillaume-Castel, R.: Observational Constraint on the Climate Sensitivity to Atmospheric CO2 Concentrations Changes Derived from the 1971–2017 Global Energy Budget, Journal of Climate, 35, 4469–4483, https://doi.org/10.1175/JCLI-D-21-0565.1, 2022.

Church, J. A., White, N. J., Konikow, L. F., Domingues, C. M., Cogley, J. G., Rignot, E., Gregory, J. M., Broeke, M. R. v. d., Monaghan, A. J., and Velicogna, I.: Revisiting the Earth's sea-level and energy budgets from 1961 to 2008, Geophysical Research Letters, 38, https://doi.org/10.1029/2011GL048794, _eprint: https://agupubs.onlinelibrary.wiley.com/doi/pdf/10.1029/2011GL048794, 2011.

Dahle, C., Flechtner, F., Gruber, C., König, D., König, R., Michalak, G., and Neumayer, K.-H.: Gfz grace level-2 processing standards document for level-2 product release 0005: revised edition, january 2013, publisher: Deutsches GeoForschungsZentrum GFZ, 2013.

Desbruyères, D., McDonagh, E. L., King, B. A., and Thierry, V.: Global and full-depth ocean temperature trends during the early twenty-first century from Argo and repeat hydrography, Journal of Climate, 30, 1985–1997, 2017.

Desbruyères, D. G., Bravo, E. P., Thierry, V., Mercier, H., Lherminier, P., Cabanes, C., Biló, T. C., Fried, N., and Femke De Jong, M.: Warming-to-Cooling Reversal of Overflow-Derived Water Masses in the Irminger Sea During 2002–2021, Geophysical Research Letters, 49, e2022GL098 057, https://doi.org/10.1029/2022GL098057, _eprint: https://onlinelibrary.wiley.com/doi/pdf/10.1029/2022GL098057, 2022.

ECCO Consortium, Fukumori, I., Wang, O., Fenty, I., Forget, G., Heimbach, P., and Ponte, R. M.: Synopsis of the ECCO central production global ocean and sea-ice state estimate (version 4 release 4), Zenodo, 2020.

Forget, G., Campin, J.-M., Heimbach, P., Hill, C., Ponte, R., and Wunsch, C.: ECCO version 4: An integrated framework for non-linear inverse modeling and global ocean state estimation, Geoscientific Model Development, 8, 3071–3104, publisher: Copernicus GmbH, 2015.

Frederikse, T., Riva, R. E. M., and King, M. A.: Ocean Bottom Deformation Due To Present-Day Mass Redistribution and Its Impact on Sea Level Observations, Geophysical Research Letters, 44, 12,306–12,314, https://doi.org/https://doi.org/10.1002/2017GL075419, _eprint: https://agupubs.onlinelibrary.wiley.com/doi/pdf/10.1002/2017GL075419, 2017.

Gaillard, F., Reynaud, T., Thierry, V., Kolodziejczyk, N., and Schuckmann, K. v.: In Situ–Based Reanalysis of the Global Ocean Temperature and Salinity with ISAS: Variability of the Heat Content and Steric Height, Journal of Climate, 29, 1305–1323, https://doi.org/10.1175/JCLI-D-15-0028.1, publisher: American Meteorological Society Section: Journal of Climate, 2016.

Gnanadesikan, A.: A simple predictive model for the structure of the oceanic pycnocline, Science, 283, 2077–2079, publisher: American Association for the Advancement of Science, 1999.

https://doi.org/10.5194/essd-2023-236
Preprint. Discussion started: 26 July 2023

Good, S. A., Martin, M. J., and Rayner, N. A.: EN4: Quality controlled ocean temperature and salinity profiles and monthly objective analyses with uncertainty estimates, Journal of Geophysical Research: Oceans, 118, 6704–6716, https://doi.org/https://doi.org/10.1002/2013JC009067, _eprint: https://agupubs.onlinelibrary.wiley.com/doi/pdf/10.1002/2013JC009067, 2013.

Gregory, J. M., Griffies, S. M., Hughes, C. W., Lowe, J. A., Church, J. A., Fukimori, I., Gomez, N., Kopp, R. E., Landerer, F., Cozannet, G. L., Ponte, R. M., Stammer, D., Tamisiea, M. E., and van de Wal, R. S. W.: Concepts and Terminology for Sea Level: Mean, Variability and Change, Both Local and Global, Surveys in Geophysics, 40, 1251–1289, https://doi.org/10.1007/s10712-019-09525-z, 2019.

Hakuba, M. Z., Frederikse, T., and Landerer, F. W.: Earth's Energy Imbalance From the Ocean Perspective (2005–2019), Geophysical Research Letters, 48, e2021GL093 624, https://doi.org/10.1029/2021GL093624, _eprint: https://onlinelibrary.wiley.com/doi/pdf/10.1029/2021GL093624, 2021.

Kato, S., Rose, F. G., Rutan, D. A., Thorsen, T. J., Loeb, N. G., Doelling, D. R., Huang, X., Smith, W. L., Su, W., and Ham, S.-H.: Surface Irradiances of Edition 4.0 Clouds and the Earth's Radiant Energy System (CERES) Energy Balanced and Filled (EBAF) Data Product, Journal of Climate, 31, 4501–4527, https://doi.org/10.1175/JCLI-D-17-0523.1, publisher: American Meteorological Society Section: Journal of Climate, 2018.

Kolodziejczyk, N., Prigent-Mazella, A., and Gaillard, F.: ISAS temperature and salinity gridded fields, https://doi.org/10.17882/52367, 2021.

Legeais, J.-F., Meyssignac, B., Faugère, Y., Guerou, A., Ablain, M., Pujol, M.-I., Dufau, C., and Dibarboure, G.: Copernicus Sea Level Space Observations: A Basis for Assessing Mitigation and Developing Adaptation Strategies to Sea Level Rise, Frontiers in Marine Science, 8, https://www.frontiersin.org/article/10.3389/fmars.2021.704721, 2021.

Levitus, S., Antonov, J. I., Boyer, T. P., Locarnini, R. A., Garcia, H. E., and Mishonov, A. V.: Global ocean heat content 1955-2008 in light of recently revealed instrumentation problems: GLOBAL OCEAN HEAT CONTENT, Geophysical Research Letters, 36, n/a–n/a, https://doi.org/10.1029/2008GL037155, 2009.

Levitus, S., Antonov, J. I., Boyer, T. P., Baranova, O. K., Garcia, H. E., Locarnini, R. A., Mishonov, A. V., Reagan, J. R., Seidov, D., Yarosh, E. S., and Zweng, M. M.: World ocean heat content and thermosteric sea level change (0–2000 m), 1955–2010, Geophysical Research Letters, 39, https://doi.org/10.1029/2012GL051106, _eprint: https://agupubs.onlinelibrary.wiley.com/doi/pdf/10.1029/2012GL051106, 2012.

Lickley, M. J., Hay, C. C., Tamisiea, M. E., and Mitrovica, J. X.: Bias in Estimates of Global Mean Sea Level Change Inferred from Satellite Altimetry, Journal of Climate, 31, 5263–5271, https://doi.org/10.1175/JCLI-D-18-0024.1, 2018.

Llovel, W. and Lee, T.: Importance and origin of halosteric contribution to sea level change in the southeast Indian Ocean during 2005–2013, Geophysical Research Letters, 42, 1148–1157, https://doi.org/https://doi.org/10.1002/2014GL062611, _eprint: https://agupubs.onlinelibrary.wiley.com/doi/pdf/10.1002/2014GL062611, 2015.

L'Ecuyer, T. S., Beaudoing, H. K., Rodell, M., Olson, W., Lin, B., Kato, S., Clayson, C. A., Wood, E., Sheffield, J., Adler, R., Huffman, G., Bosilovich, M., Gu, G., Robertson, F., Houser, P. R., Chambers, D., Famiglietti, J. S., Fetzer, E., Liu, W. T., Gao, X., Schlosser, C. A., Clark, E., Lettenmaier, D. P., and Hilburn, K.: The Observed State of the Energy Budget in the Early Twenty-First Century, Journal of Climate, 28, 8319–8346, https://doi.org/10.1175/JCLI-D-14-00556.1, publisher: American Meteorological Society Section: Journal of Climate, 2015.

Magellium/LEGOS: Atlantic OHC from space: Heat content change over the Atlantic Ocean by space geodetic approach, https://doi.org/10.24400/527896/A01-2022.012, artwork Size: 35 Mo Pages: 35 Mo, 2022.

https://doi.org/10.5194/essd-2023-236
Preprint. Discussion started: 26 July 2023

Marti, F., Blazquez, A., Meyssignac, B., Ablain, M., Barnoud, A., Fraudeau, R., Jugier, R., Chenal, J., Larnicol, G., Pfeffer, J., Restano, M., and Benveniste, J.: Monitoring the ocean heat content change and the Earth energy imbalance from space altimetry and space gravimetry, Earth System Science Data, 14, 229–249, https://doi.org/10.5194/essd-14-229-2022, 2022.

Mayer, J., Mayer, M., Haimberger, L., and Liu, C.: Comparison of Surface Energy Fluxes from Global to Local Scale, Journal of Climate, 35, 4551–4569, https://doi.org/10.1175/JCLI-D-21-0598.1, publisher: American Meteorological Society Section: Journal of Climate, 2022.

McDougall, T. and Barker, P.: Getting started with TEOS-10 and the Gibbs Seawater (GSW) Oceanographic Toolbox, http://teos-10.org/pubs/Getting_Started.pdf, mcDougall, T.J. and P.M. Barker, 2011: Getting started with TEOS-10 and the Gibbs Seawater (GSW) Oceanographic Toolbox, 28pp., SCOR/IAPSO WG127, ISBN 978-0-646-55621-5., 2011.

Mercier, H., Lherminier, P., and Pérez, F. F.: The Greenland-Portugal Go-Ship A25 OVIDE CTDO2 hydrographic data, https://doi.org/10.17882/46448, 2022.

Meyssignac, B., Boyer, T., Zhao, Z., Hakuba, M. Z., Landerer, F. W., Stammer, D., Köhl, A., Kato, S., L'Ecuyer, T., Ablain, M., Abraham, J. P., Blazquez, A., Cazenave, A., Church, J. A., Cowley, R., Cheng, L., Domingues, C. M., Giglio, D., Gouretski, V., Ishii, M., Johnson, G. C., Killick, R. E., Legler, D., Llovel, W., Lyman, J., Palmer, M. D., Piotrowicz, S., Purkey, S. G., Roemmich, D., Roca, R., Savita, A., Schuckmann, K. v., Speich, S., Stephens, G., Wang, G., Wijffels, S. E., and Zilberman, N.: Measuring Global Ocean Heat Content to Estimate the Earth Energy Imbalance, Frontiers in Marine Science, 6, https://doi.org/10.3389/fmars.2019.00432, publisher: Frontiers, 2019.

Palmer, M. D., Roberts, C. D., Balmaseda, M., Chang, Y.-S., Chepurin, G., Ferry, N., Fujii, Y., Good, S. A., Guinehut, S., Haines, K., Hernandez, F., Köhl, A., Lee, T., Martin, M. J., Masina, S., Masuda, S., Peterson, K. A., Storto, A., Toyoda, T., Valdivieso, M., Vernieres, G., Wang, O., and Xue, Y.: Ocean heat content variability and change in an ensemble of ocean reanalyses, Climate Dynamics, 49, 909–930, https://doi.org/10.1007/s00382-015-2801-0, 2017.

Palmer, M. D., Durack, P. J., Chidichimo, M. P., Church, J. A., Cravatte, S., Hill, K., Johannessen, J. A., Karstensen, J., Lee, T., and Legler, D.: Adequacy of the ocean observation system for quantifying regional heat and freshwater storage and change, Frontiers in Marine Science, 6, 416, publisher: Frontiers Media SA, 2019.

Palter, J. B.: The role of the Gulf Stream in European climate, Annual review of marine science, 7, 113–137, publisher: Annual Reviews, 2015.

Prandi, P., Meyssignac, B., Ablain, M., Spada, G., Ribes, A., and Benveniste, J.: Local sea level trends, accelerations and uncertainties over 1993–2019, Scientific Data, 8, 1, https://doi.org/10.1038/s41597-020-00786-7, number: 1 Publisher: Nature Publishing Group, 2021.

Rose, B. E. and Rayborn, L.: The effects of ocean heat uptake on transient climate sensitivity, Current climate change reports, 2, 190–201, publisher: Springer, 2016.

Rose, B. E., Armour, K. C., Battisti, D. S., Feldl, N., and Koll, D. D.: The dependence of transient climate sensitivity and radiative feedbacks on the spatial pattern of ocean heat uptake, Geophysical Research Letters, 41, 1071–1078, publisher: Wiley Online Library, 2014.

Ruiz-Barradas, A., Chafik, L., Nigam, S., and Häkkinen, S.: Recent subsurface North Atlantic cooling trend in context of Atlantic decadal-to-multidecadal variability, Tellus A: Dynamic Meteorology and Oceanography, 70, 1–19, https://doi.org/10.1080/16000870.2018.1481688, publisher: Taylor & Francis _eprint: https://doi.org/10.1080/16000870.2018.1481688, 2018.

Stammer, D., Balmaseda, M., Heimbach, P., Köhl, A., and Weaver, A.: Ocean Data Assimilation in Support of Climate Applications: Status and Perspectives, Annual Review of Marine Science, 8, 491–518, https://doi.org/10.1146/annurev-marine-122414-034113, _eprint: https://doi.org/10.1146/annurev-marine-122414-034113, 2016.

https://doi.org/10.5194/essd-2023-236
Preprint. Discussion started: 26 July 2023

Tang, L., Li, J., Chen, J., Wang, S.-Y., Wang, R., and Hu, X.: Seismic Impact of Large Earthquakes on Estimating Global Mean Ocean Mass Change from GRACE, Remote Sensing, 12, 935, https://doi.org/10.3390/rs12060935, number: 6 Publisher: Multidisciplinary Digital Publishing Institute, 2020.

Taylor, J. R.: An Introduction to Error Analysis: The Study of Uncertainties in Physical Measurements, University Science Books, Sausalito, California, 2nd edn., http://gen.lib.rus.ec/book/index.php?md5=cccb32c31afb10c95d5acd3586806afd, 1997.

von Schuckmann, K., Palmer, M. D., Trenberth, K. E., Cazenave, A., Chambers, D., Champollion, N., Hansen, J., Josey, S. A., Loeb, N., Mathieu, P.-P., Meyssignac, B., and Wild, M.: An imperative to monitor Earth's energy imbalance, Nature Climate Change, 6, 138, https://doi.org/10.1038/nclimate2876, 2016.

von Schuckmann, K., Cheng, L., Palmer, M. D., Hansen, J., Tassone, C., Aich, V., Adusumilli, S., Beltrami, H., Boyer, T., Cuesta-Valero, F. J., Desbruyères, D., Domingues, C., García-García, A., Gentine, P., Gilson, J., Gorfer, M., Haimberger, L., Ishii, M., Johnson, G. C., Killick, R., King, B. A., Kirchengast, G., Kolodziejczyk, N., Lyman, J., Marzeion, B., Mayer, M., Monier, M., Monselesan, D. P., Purkey, S., Roemmich, D., Schweiger, A., Seneviratne, S. I., Shepherd, A., Slater, D. A., Steiner, A. K., Straneo, F., Timmermans, M.-L., and Wijffels, S. E.: Heat stored in the Earth system: where does the energy go?, Earth System Science Data, 12, 2013–2041, https://doi.org/https://doi.org/10.5194/essd-12-2013-2020, publisher: Copernicus GmbH, 2020.

Wong, A. P. S., Wijffels, S. E., Riser, S. C., Pouliquen, S., Hosoda, S., Roemmich, D., Gilson, J., Johnson, G. C., Martini, K., Murphy, D. J., Scanderbeg, M., Bhaskar, T. V. S. U., Buck, J. J. H., Merceur, F., Carval, T., Maze, G., Cabanes, C., André, X., Poffa, N., Yashayaev, I., Barker, P. M., Guinehut, S., Belbéoch, M., Ignaszewski, M., Baringer, M. O., Schmid, C., Lyman, J. M., McTaggart, K. E., Purkey, S. G., Zilberman, N., Alkire, M. B., Swift, D., Owens, W. B., Jayne, S. R., Hersh, C., Robbins, P., West-Mack, D., Bahr, F., Yoshida, S., Sutton, P. J. H., Cancouët, R., Coatanoan, C., Dobbler, D., Juan, A. G., Gourrion, J., Kolodziejczyk, N., Bernard, V., Bourlès, B., Claustre, H., D'Ortenzio, F., Le Reste, S., Le Traon, P.-Y., Rannou, J.-P., Saout-Grit, C., Speich, S., Thierry, V., Verbrugge, N., Angel-Benavides, I. M., Klein, B., Notarstefano, G., Poulain, P.-M., Vélez-Belchí, P., Suga, T., Ando, K., Iwasaska, N., Kobayashi, T., Masuda, S., Oka, E., Sato, K., Nakamura, T., Sato, K., Takatsuki, Y., Yoshida, T., Cowley, R., Lovell, J. L., Oke, P. R., van Wijk, E. M., Carse, F., Donnelly, M., Gould, W. J., Gowers, K., King, B. A., Loch, S. G., Mowat, M., Turton, J., Rama Rao, E. P., Ravichandran, M., Freeland, H. J., Gaboury, I., Gilbert, D., Greenan, B. J. W., Ouellet, M., Ross, T., Tran, A., Dong, M., Liu, Z., Xu, J., Kang, K., Jo, H., Kim, S.-D., and Park, H.-M.: Argo Data 1999–2019: Two Million Temperature-Salinity Profiles and Subsurface Velocity Observations From a Global Array of Profiling Floats, Frontiers in Marine Science, 7, https://www.frontiersin.org/article/10.3389/fmars.2020.00700, 2020.